Available online at www.sciencedirect.com
ScienceDirect
Journal of Power Sources 179 (2008) 407–411
JOURNAL OF POWER SOURCES
www.elsevier.com/locate/jpowsour

Short communication

A novel high capacity, environmentally benign energy storage system: Super-iron boride battery

Xingwen Yu [a,*], Stuart Licht [b]

[a] *Department of Chemical and Biological Engineering, The University of British Columbia, 2360 East Mall, Vancouver, BC, Canada V6T 1Z3*
[b] *Department of Chemistry, University of Massachusetts, 100 Morrissey Blvd, Boston, MA 02125, USA*

Received 23 November 2007; received in revised form 17 December 2007; accepted 18 December 2007
Available online 26 December 2007

Abstract

High electrochemical capacity of alkaline boride anodes is presented. The alkaline anodes based on transition metal borides (demonstrated with TaB, TaB_2, TiB_2 and VB_2) can deliver exceptionally high discharge capacity. Over 2000 and 3800 mAh g^{-1} discharge capacities are obtained for the commercially available TiB_2 and VB_2 respectively, much higher than the theoretical capacity of commonly used zinc metal (820 mAh g^{-1}) alkaline anode. Coupling with the super-iron cathodes, the novel Fe^{6+}/B^{2-} battery chemistry generates a matched electrochemical potential to the conventional MnO_2–Zn battery, but sustains a much higher electrochemical capacity. High capacity TiB_2 and VB_2 anodes are further studied by coupling with a variety of cathodes (such as MnO_2, NiOOH, KIO_4 and composite K_2FeO_4/AgO). Both TiB_2 and VB_2 show good compatibilities with each of these cathodes. With the additive AgO to the super-iron (K_2FeO_4) cathode, a K_2FeO_4/AgO composite cathode TiB_2 anode alkaline battery exhibits high-rate discharge performance.

Keywords: Boride anodes; Super-iron boride battery; High capacity; K_2FeO_4/AgO cathode

1. Introduction

Alkaline Zn–MnO_2 redox charge storage has been established for over a century. Among the different types of aqueous primary batteries available in the market, the Zn–MnO_2 system has been possessing a dominant share because of its appropriate performance and low cost. However, this battery chemistry is increasingly limited in meeting the growing energy and power demands of contemporary consumer devices. Therefore, the search for new energy storage chemistry systems with higher capacity and energy density is a continuous need. A number of new materials, such as metal hydride and intercalation compounds have been successfully applied to the high performance Ni–MH and Li-ion batteries [1,2]. We introduced a new battery type, super-iron battery based on the high Fe(VI) cathodic charge storage in 1999 [3]. Followed the primary alkaline super-iron batteries, recently, rechargable thin layer super-iron cathode [4,5] and high performance composite Fe(VI)/AgO cathode [6] have also been successfully developed. In 2004, it was reported that metal borides could be used as anodic alkaline charge storage materials [7,8]. Representative transition metal borides include TiB_2 and VB_2 which can store several folds more charge than a zinc anode through multi-electron charge transfer. Corresponding anodic reactions are: [7]

$$TiB_2 + 12OH^- \rightarrow Ti(amorphous) + 2{BO_3}^{3-} + 6H_2O + 6e^- \quad (1)$$

$$VB_2 + 20OH^- \rightarrow {VO_4}^{3-} + 2{BO_3}^{3-} + 10H_2O + 11e^- \quad (2)$$

However, one obstacle was evident towards implementation of this alkaline boride (MB_2, M = Ti or V) anodic chemistry. The electrochemical potential of the boride anodes was more positive than that of zinc. Therefore, the voltage of a boride MnO_2 cell was low compared to the voltage of the pervasive Zn–MnO_2 battery. In our recent communication [9], we introduced a novel Fe^{6+}/B^{2-} battery chemistry in which the super-iron (Fe^{6+}) cathode provides the requisite additional electrochemical potential

* Corresponding author. Tel.: +1 604 728 8895.
E-mail address: xingwenyu@yahoo.com (X. Yu).

0378-7753/$ – see front matter © 2007 Elsevier B.V. All rights reserved.
doi:10.1016/j.jpowsour.2007.12.060

for the boride (B^{2-}) anode. Therefore, the Fe(VI)–MB_2 couple generates a similar potentials to the Zn–MnO_2 battery. In addition, the obstacles of the boride anode decomposition are overcome by applying a zirconia hydroxide-shuttle overlayer on the anode particle surface [9]. This paper is a continuous study of the Fe^{6+}/B^{2-} redox chemistry. More boride anodes and more alkaline cathodes, especially Fe(VI)/AgO composite cathode are studied in super-iron boride batteries.

2. Experimental

Cathode materials used in this study include MnO_2 (EMD, EraChem K60), NiOOH (taken from the commercial Ni–MH button cell (Powerstream®)), KIO_4 (from ACROS®) and the lab synthesized K_2FeO_4, AgO. Preparation and analysis of K_2FeO_4 has been detailed elsewhere [10,11]. K_2FeO_4 of 97–98.5% is prepared according to:

$$Fe(NO_3)_3{\cdot}9H_2O + 3/2KClO + 5KOH \rightarrow K_2FeO_4 + 3/2KCl + 3KNO_3 + 23/2H_2O \quad (3)$$

AgO is prepared by standard methods [12] (the reaction at 85 °C of an alkaline $AgNO_3$ solution with $K_2S_2O_8$) in accord with:

$$4AgNO_3 + 2K_2S_2O_8 + 8NaOH \rightarrow 4AgO + K_2SO_4 + 3Na_2SO_4 + 2NaNO_3 + 2KNO_3 + 4H_2O \quad (4)$$

Anode materials TiB_2 (10 μm powder), VB_2 (325 mesh powder) TaB (325 mesh), TaB_2 (325 mesh), MgB_2 (325 mesh), CrB_2 (325 mesh), CoB_2 (325 mesh), Ni_2B (powder, 30 mesh) and LaB_6 (powder, 10 μm) are from Aldrich®.

Batteries studied in this paper are prepared as 1 cm button cell configuration. The cells are prepared with a saturated KOH electrolyte. Preparation of the cathodes and anodes will be detailed in Section 3. Conductive medium used in cathode and anode preparation is 1 μ graphite (Leico Industries Inc.). The cells are discharged at a constant load (will be indicated in Section 3). Primary discharge is measured as the cell potential variation over time, and is recorded with LabView Acquisition on a PC, and cumulative discharge, as milliampere hours, determined by subsequent integration.

3. Results and discussion

From the thermodynamic view [13], a lot of transition metals, such as Ti, V, Mn, and Fe, and non-metal elements such as B, C, and Si have larger theoretical electrochemical capacity or more negative electrode potentials and should be capable of performing as competitive high energy anode materials for batteries. However, chemical instability or surface passivation of these elements limits their use of delivering electrochemical capacities as anode materials in batteries. Many transition metal borides have thermodynamic parameters and electronic conductivities similar to those of the corresponding transition metals. Therefore, from the electrochemical energy conversion viewpoint, transition metal borides may constitute a large class of promising electrochemically active materials for batteries [14,15]. In the study herein, various transition metal borides TaB, TaB_2, MgB_2, CrB_2, CoB_2, Ni_2B, LaB_6, TiB_2 and VB_2 are considered as the anodes for alkaline battery. Similarly as TiB_2 and VB_2 [7], electrochemical potentials of the borides are more positive than zinc metal, thus the cell voltage of MnO_2-boride batteries are lower than the conventional MnO_2–Zn battery. The alkaline thermodynamic potential of the $3e^-$ reduction of super-iron cathodes Fe(VI → III) via Eq. (5), is approximately 250 mV higher than the one electron reduction of MnO_2 via Eq. (6), with potentials reported versus SHE (the standard H_2 electrode):

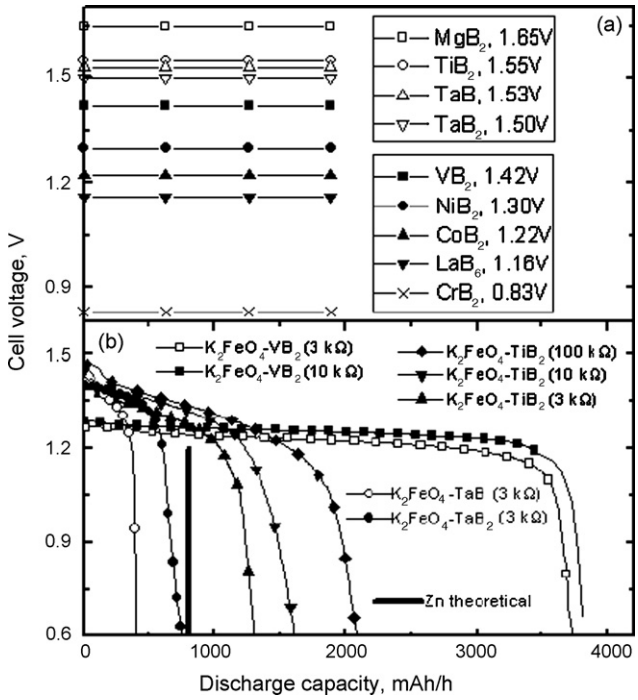

Fig. 1. (a): Open circuit potentials (OCP) of various boride anodes alkaline super-iron (K_2FeO_4) cathode batteries. Electrolyte used is saturated KOH. (b): Discharge profiles of TaB, TaB_2, TiB_2 and VB_2–K_2FeO_4 alkaline cells.

$$FeO_4^{2-} + 5/2H_2O + 3e^- \rightarrow 1/2Fe_2O_3 + 5OH^-; \quad E = 0.60\,V \quad (5)$$

$$MnO_2 + 1/2H_2O + e^- \rightarrow 1/2Mn_2O_3 + OH^-; \quad E = 0.35\,V \quad (6)$$

Coupling with super-iron cathode (K_2FeO_4), open circuit potentials of these super-iron boride batteries are presented in Fig. 1a.

In addition to the previously studied TiB_2 and VB_2 [7,9], in Fig. 1a, only tantalum boride salts exhibit a degree of anodic charge storage, each of the other borides did not exhibit significant primary discharge behavior due to their high solubilities in alkaline solution or their reaction with alkaline electrolyte. As previously reported [7,9], the alkaline oxidation of the TiB_2

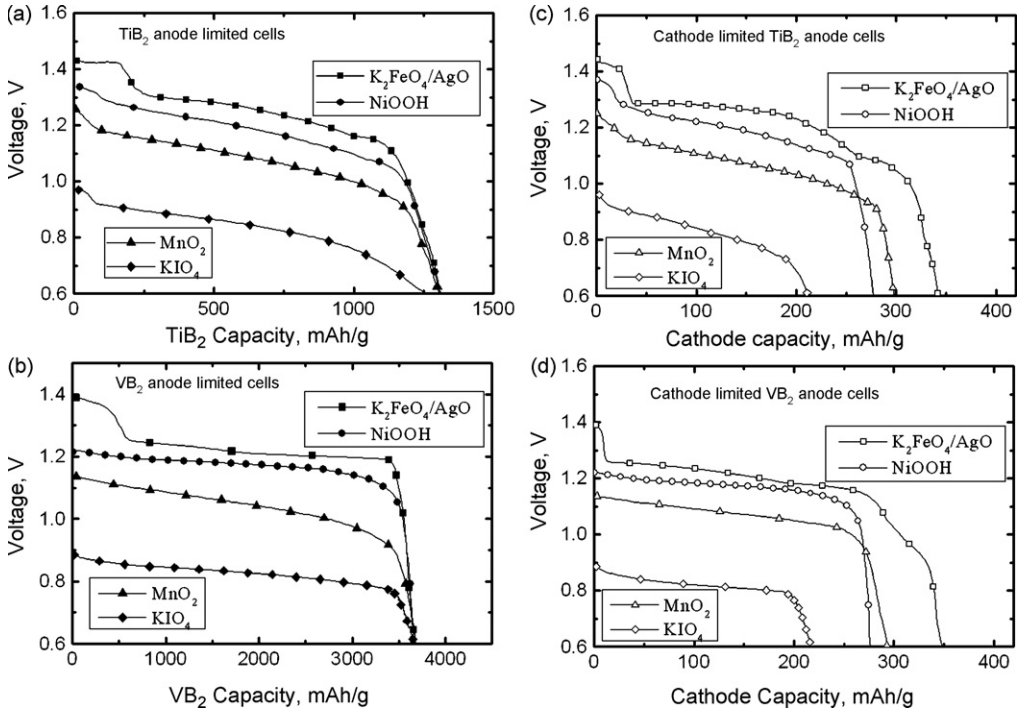

Fig. 2. Comparative discharges of titanium (top) or vanadium (bottom) boride anode alkaline batteries with a variety of cathodes, under (left) anode-limited or (right) cathode-limited conditions. The cells are discharged at a constant 3 kΩ load. The cathode is either 76.5% K_2FeO_4, 8.5% AgO, 5% KOH and 10% 1 μm graphite; or 90% MnO_2 and 10% 1 μm graphite; or 90% NiOOH and 10% 1 μm graphite; or 75% KIO_4 and 25% 1 μm graphite. Anode- or cathode-limited conditions are studied by packing each cell, respectively, with excess intrinsic cathode or anode capacity. Electrolyte used is saturated KOH.

anode produced amorphous titanium, and similarly we expect the reduction of TaB_2 can yield tantalum:

$$TaB_2 + 12OH^- \rightarrow Ta + 2BO_3^{3-} + 6H_2O + 6e^- \quad (7)$$

$$TaB + 6OH^- \rightarrow Ta + BO_3^{3-} + 3H_2O + 3e^- \quad (8)$$

According to the oxidation reaction of the half cell and the formula weight of TaB_2 (FW 202.57 g mol^{-1}) or TaB (FW 191.76 g mol^{-1}), intrinsic capacity of TaB_2 and TaB would accordingly be: 794 and 419 mAh g^{-1}.

Discharge profiles of TaB and TaB_2 anode, K_2FeO_4 cathode button cells are shown in Fig. 1b. Button cells are prepared with excess cathode capacity and discharged at a low current to probe the anode's limits and characteristics. As seen in the figure, the TaB_2 exhibits an anodic storage capacity comparable to the widely used conventional alkaline zinc anode (820 mAh g^{-1}). Compared to the theoretical capacity (794 mAh g^{-1} for TaB_2 and 419 mAh g^{-1} for TaB), 88% for TaB_2 and 93% for TaB of the coulombic efficiency are obtained for these two anodes. The discharge of TiB_2, rather than TaB_2, to the amorphous metal product is comparable to a significantly higher gravimetric charge storage capacity due to the lighter weight of this metal (47.87 g titanium mol^{-1} compared to 180.95 g tantalum mol^{-1}), in accord with Eq. (1). As seen in Fig. 1b, a significant advantage of the titanium boride anode is the higher capacity compared to the conventional alkaline zinc anode (820 mAh g^{-1}). The TiB_2 anode discharge is in excess of 1300 mAh g^{-1} at moderate discharge rates (3 kΩ load) and is in excess of 2000 mAh g^{-1} at low discharge rates (100 kΩ load). In accord with Eq. (1), and a formula weight, $W = 69.5$ g mol^{-1}, TiB_2, has a net intrinsic 6 electron anodic capacity of $6F/W = 2314$ mAh g^{-1} (F = the faraday constant). While the TiB_2 exhibits greater intrinsic capacity than the TaB_2, a vanadium, compared to a titanium, diboride salt can yield even higher alkaline anodic capacity. Unlike TiB_2, the alkaline VB_2 anode undergoes an oxidation of both the boron and the tetravalent transition metal ion, with a net 11 electron process. In accord with Eq. (2), VB_2, will have an intrinsic anodic capacity of $11F/(W = 72.6$ g mol$^{-1}) = 4060$ mAh g^{-1}, rivaling the high anodic capacity of lithium (3860 mAh g^{-1}). As evident in Fig. 1b, this substantial capacity of VB_2 is experimentally realized (3800 mAh g^{-1}) in the discharge of the alkaline super-iron VB_2 cell. The VB_2 sustains more efficient higher rate discharge (and lower polarization loss) than the TiB_2 alkaline anode cell. As seen comparing the 3 kΩ discharges in Fig. 1b, the TiB_2 discharge sustains 56% of the intrinsic capacity, whereas the VB_2 sustains 91% of the intrinsic capacity (which increases to 94% during a 10 kΩ discharge).

Fig. 2 probes the boride anode cells, not only under anode-limited, but also with a variety of cathode-limited conditions. K_2FeO_4 has an intrinsic three electron cathodic storage capacity of $3F/(W = 198$ g mol$^{-1}) = 406$ mAh g^{-1}, compared to the capacity of MnO_2 (308 mAh g^{-1}). Recently, it has been shown that hydroxide and Ag(II) additions mediate Fe(VI) charge transfer [6]. Consistent with this observation, in lieu of the pure K_2FeO_4 salt utilized in Fig. 1 (75% K_2FeO_4/25% graphite cathode), the K_2FeO_4 cathode in Fig. 2 includes AgO and KOH. This permits the Fe(VI) cathode to sustain higher current densities, and greater depth of discharge, with significantly less

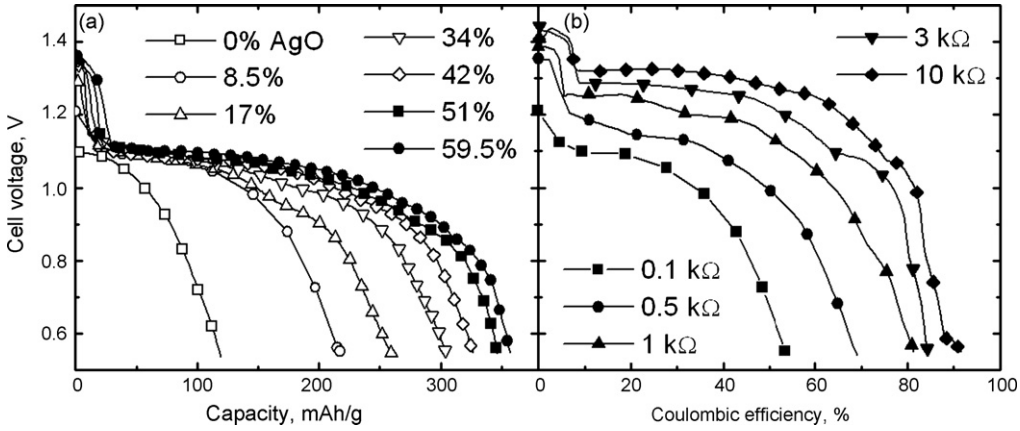

Fig. 3. (a): High current discharge profiles of composite K_2FeO_4/AgO–TiB_2 button cells. The K_2FeO_4/AgO composite cathode is studied in cells with excess intrinsic anode capacity, in a 1 cm coin cell, discharged under 0.1 kΩ constant load conditions. Fraction of AgO additive is from 0% to 59.5%. (b): Discharge voltage profiles at a range of discharge loads, of fixed composition composite K_2FeO_4/AgO–TiB_2 button cells. Electrolyte used is saturated KOH.

graphite added as a conductive matrix, and the cathode contains in addition to a K_2FeO_4 salt, 8.5% AgO, 5% KOH and only 10% graphite. Other alkaline cathodes compared in Fig. 2 include the conventional MnO_2 and NiOOH alkaline electrodes, and a recently introduced periodate (KIO_4) cathode [16]. The highest cathodic capacity is that of the Fe(VI) cathode, as shown on the right side (top and bottom) of Fig. 2, and also evident is the higher discharge potential, compared to cells with alternate alkaline cathodes in the boride cells.

The small voltage plateau evident in Fig. 2, during the initial discharge of the Fe(VI) cathode, is largely due to the Ag(II ⇒ I) reduction of the added AgO. In addition, the voltage plateaus are visible for each of the non-Fe(VI)/TiB_2 cells, during the initial discharge, (Fig. 2 top, left and right), but not evident in the VB_2 cells (bottom, left and right), are consistent with complexities attributed to the simultaneous Ti(VI) reduction [7]. In alkaline MnO_2/zinc cells, the MnO_2 cathode exhibits a steep voltage decrease with increasing depth of discharge. This voltage loss increases significantly with increasing discharge rate, and decreases the high-rate storage capacity of alkaline MnO_2/zinc cells. The alkaline NiOOH cathode exhibits less of this voltage loss, and similarly the $3e^-$ alkaline discharge profile of Fe(VI) is flat. The alkaline MnO_2/boride cell also exhibits the typical MnO_2 voltage drop in Fig. 2. As noted in Fig. 1, VB_2 anodes exhibit less polarization loss than TiB_2, and as seen on the left bottom of Fig. 2, in conjunction with a VB_2 anode, the NiOOH and Fe(VI) cathodes exhibit significantly less voltage drop with increasing depth of discharge, than with a MnO_2 cathode.

Specially, $Fe^{6+}(Ag^{2+})/B^{2-}$ alkaline battery, with K_2FeO_4/AgO composite cathode and TiB_2 anode is further probed. AgO additive facilitates the Fe(VI) charge transfer. Increasing a AgO additive in a composite K_2FeO_4 cathode remarkably improves its charge transfer at high discharge rate, as shown in Fig. 3a.

With a large fraction of AgO additive, the composite cathode yields over four times capacity than that without AgO additive. An effective composite cathode is prepared with 29.5 mg 76.5% K_2FeO_4, 8.5% AgO, 5% KOH and 10% graphite. Excess capacity TiB_2 anode is prepared as 75% TiB_2, 20% graphite, 4.5% KOH and 0.5% bender (T-30, 30% teflon). Discharge profiles of this novel type of button cells at different constant loads are shown in Fig. 3b. The intrinsic capacity of the composite cathode is 408 mAh g^{-1}, based on 3-electron charge transfer of K_2FeO_4 (406 mAh g^{-1}) and $2e^-$ charge transfer of AgO (432 mAh g^{-1}) (90% × 406 + 10% × 432 = 408 mAh g^{-1}). Depth of discharge of this composite cathode is relatively high at low current density discharge, and utilization of intrinsic capacity is over 80% (e.g. Discharged at 3000 and 10,000 Ω). However, only 45% of capacity is utilized at lower load, 100 Ω, discharge.

The range from maximum experimental (<160 mA g^{-1}) to theoretical ($2F$ per Zn + $2MnO_2$ = 222 mAh g^{-1}) charge storage capacities of the conventional alkaline Zn–MnO_2 cell are shown as vertical lines in Fig. 4. The theoretical capacities for the complete super-iron TaB_2 ($6F$ per $TaB_2 + 2K_2FeO_4$) and super-iron TaB ($3F$ per $TaB + 1K_2FeO_4$) are respectively at 268 and 206 mAh g^{-1}. Theoretical capacities for the complete super-iron TiB_2 ($6F$ per $TiB_2 + 2K_2FeO_4$) and super-iron VB_2 ($11F$ per $VB_2 + 11/3K_2FeO_4$) are higher respectively at 345 and 369 mAh g^{-1}. The discharge of the complete super-iron boride redox chemistry is investigated in Fig. 4 using cells

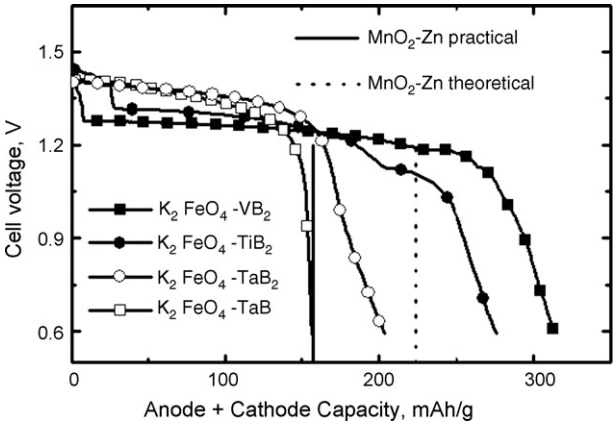

Fig. 4. Combined (anode + cathode) capacity comparison of the super-iron boride alkaline batteries to the conventional (MnO_2/Zn) alkaline battery. Electrolyte used is saturated KOH.

with balanced anode and cathode capacity (based on the intrinsic capacity of the anode and cathode components). As seen in Fig. 4, the super-iron titanium boride cell combined anode and cathode capacity is experimentally in excess of 250 mAh g^{-1}, and that of the super-iron VB_2 cell is over 310 mAh g^{-1}, which is two-fold higher than that of the conventional alkaline battery chemistry (MnO_2/Zn). The combined super-iron tantalum boride cells also yield high practical capacity comparable to that of Zn–MnO_2 cell. The super-iron boride chemistry exhibits significantly higher charge storage than conventional alkaline primary storage chemistry. A further optimization of both the boride and super-iron particle size should further enhance cell performance.

4. Conclusions

A novel high capacity battery chemistry based on super-iron cathode and transition metal boride anode is presented. This Fe^{6+}/B^{2-} redox chemistry generates a matched electrochemical potential to the conventional MnO_2–Zn battery chemistry, but sustains a much higher electrochemical capacity. With the additive AgO to the super-iron (K_2FeO_4) cathode, a K_2FeO_4/AgO composite cathode TiB_2 anode alkaline battery exhibits high-rate discharge performance. High capacity TiB_2 and VB_2 anodes are also compatible to variety of other alkaline cathodes, such as commonly used cathodes MnO_2, NiOOH and new reported KIO_4.

References

[1] S.R. Ovshinsky, M.A. Fetcenko, J. Ross, Science 260 (1993) 176.
[2] G.M. Julien, Mater. Sci. Eng. R 40 (2003) 47.
[3] S. Licht, B. Wang, S. Ghosh, Science 285 (1999) 1039.
[4] S. Licht, Ran Tel-Vered, Chem. Commun. 6 (2004) 628.
[5] S. Licht, C. DeAlwis, J. Phys. Chem. B 110 (2006) 12394.
[6] S. Licht, X. Yu, D. Zheng, Chem. Commun. 41 (2006) 4341.
[7] H.X. Yang, Y.D. Wang, X.P. Ai, C.S. Cha, Electrochem. Solid-State Lett. 7 (2004) A212.
[8] Y.D. Wang, X.P. Ai, Y.L. Cao, H.X. Yang, Electrochem. Commun. 6 (2004) 780.
[9] S. Licht, X. Yu, D. Qu, Chem. Commun. 26 (2007) 2753.
[10] S. Licht, V. Naschitz, B. Liu, S. Ghosh, N. Halperin, L. Halperin, D. Rozen, J. Power Sources 99 (2001) 7.
[11] S. Licht, V. Naschitz, L. Halperin, N. Halperin, L. Lin, J. Chen, S. Ghosh, B. Liu, J. Power Sources 101 (2001) 167.
[12] S. Licht, V. Naschitz, S. Ghosh, J. Phys. Chem. B 106 (2002) 5947.
[13] A.J. Bard, R. Parsons, J. Jordan, Standard Potentials in Aqueous Solutions, Marcel Dekker, New York, 1985, p. 798.
[14] S. Amendola, U.S. Patent 5 948 558 (1999).
[15] S. Amendola, U.S. Patent 6 468 694 (2002).
[16] S. Licht, X. Yu, Electrochem. Solid-State Lett. 10 (2007) A36.